Comparison of reduced models for plasma turbulence in high β conditions

Felix Watts[1,2], David Dickinson[1], Francis Casson[2], William Hornsby[2], Harry Dudding[2], Bhavin Patel[2], Daniel Kennedy[2]
[1]York Plasma Institute, University of York, [2]UKAEA (United Kingdom Atomic Energy Authority)

Abstract

Spherical tokamaks offer numerous benefits over conventional tokamaks, including enhanced MHD stability, access to a higher ratio of plasma pressure to magnetic pressure β, and reduced reactor size [1, 2]. Current and future spherical tokamaks include MAST-U, NSTX-U, and the UK's planned spherical tokamak for energy production (STEP).

The linear performance of Gyro-fluid code (TGLF) in the electromagnetic turbulence dominated regions found in STEP like conditions is assessed[3]. Tuning of TGLF numerical settings via fixing the width search at a valued of 1.3 removed spurious high growth rate KBMs that commonly occurr in high β conditions. The existing quasi-linear saturation rules were then tested in high β ST turbulence, including the effects of flow shear stabilisation. It was found that the new numerical settings for TGLF (TGLF V3) improved quantitative agreement in heat flux prediction as well as more closely matching the amount of $E \times B$ shear required for the suppression of turbulence.

1 TGLF

Non-linear gyrokinetic codes can successfully predict turbulent fluxes in high β regimes, but are far too computationally costly to be used in the integrated modelling workflows necessary to identify steady state plasma scenarios for STEP [4]. Quasi-linear codes, such as the gyrofluid model (TGLF) [5] couple a model of the linear properties of micro turbulent instabilities, such as Kinetic Ballooning Modes (KBMs), with a saturation rule, which predicts the maximum amplitude of these instabilities. Both reduced linear models and saturation rules commonly include numerical parameters fitted for specific plasma conditions. Refitting these numerical parameters for high β conditions is expected to improve performance. A Hermite basis function is obtained by multiplying the corresponding Hermite polynomials by the square root for the Gaussian measure with respect to which the Hermite polynomials are orthogonal.

$$\Psi_n = e^{-\hat{\theta}^2/2} h_n, \quad \int_{-\infty}^{\infty} d\hat{\theta}\, \Psi_m \Psi_n = \delta_{n,m}, \quad \hat{\theta} = \theta/\theta_w. \tag{1}$$

In TGLF the gyro fluid equations are solved as an eigenvalue problem using these Hermite basis functions. The gyro fluid equations are converted from θ space by taking the inner product with Hermite Basis functions. Then an integration is performed using a Gauss-Hermite Quadrature. The number of nodes used in this is determined by the TGLF numerical parameter `NXGRID`.

Initially TGLF fits the instability eigenfunction with `NBASIS_MIN` (default 2) Hermite basis functions, and the width of the Gaussian measure θ_w is adjusted between `WIDTH_MIN` and `WIDTH_MAX`, considering the electrostatic only (ES) or all fields (EM) to get the maximum growth rate. Hermite Basis functions up to `NBASIS_MAX` are added to better resolve the eigenfunction. The TGLF numerical parameter

FILTER determines how high-frequency modes are removed, as spurious modes caused by numerical artifacts can occur [6]. THETA_TRAPPED sets the boundary for trapped particles to be treated as either Landau averaging, or resonant. In previous work by B.Patel et al, reducing THETA_TRAPPED from its default of 0.7 to 0.4, improved growth rate predictions in high β conditions [7]. In this work, the best agreement was found returning to the default value of 0.7.

2 Profiles

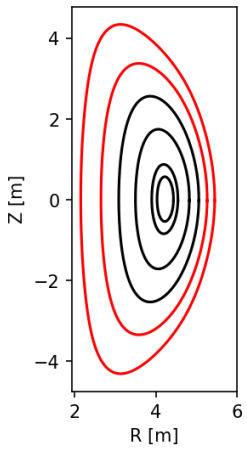

Figure 1: Plot of the magnetic flux surfaces for the T3D relaxed STEP-EC-HD case, with the specific radial cases used in R3 ($\rho = 0.655$) and R4 ($\rho = 0.818$) shown in red

Three STEP profiles and one MAST-U profile are chosen for Analysis. The STEP-EC-HD case was designed using the integrated modelling code JINTRAC [8] which uses the empirical Bohm-Gyro-Bohm model for transport calculations. It was designed for a fusion output of $P_{fus} \sim 1.8GW$ and utilises only electron cyclotron current drive heating

The profile was put into the transport solver T3D utilising a quasilinear model designed for high β plasmas on top of the linear gyrokinetic code GS2 [9]. This resulted in the electron and ion temperature gradients for the STEP-EC-HD cases being relaxed to a transport steady state. Two radial cases of the relaxed case are considered with ρ values of 0.655 and 0.818. The flux surfaces corresponding to these ρ values are shown in Fig. 1

Finally, the MAST-U pulse 48567 during its flat-top, 531ms into the pulse was considered. This case was chosen due to it's high β and lack of MHD instabilities and has been analysed in depth.

	GP_Model	MAST-U_48567	R3	R4	S1
shift	-0.440	-0.368	-0.406	-0.505	-0.399
ρ	0.670	0.718	0.655	0.818	0.637
κ	2.660	1.760	2.560	2.610	2.560
κ'	-0.0633	0.088	0.015	0.194	0.015
δ	0.333	0.168	0.294	0.402	0.283
δ'	0.168	0.200	0.432	0.922	0.292
q	[2- 9]	**−2.39**	3.580	5.310	3.490
$\hat{s}$	[0-5]	1.630	1.160	1.970	1.200
β	[0-0.3]	0.036	0.095	0.053	0.010
β'	†	-0	-0.262	-0.758	-0.056
a/L_T (D)	[0-8]	3.240	0.790	4.240	1.820
a/L_T (E)	[0-8]	3.260	1.590	2.210	1.580
a/L_n (E)	[0-6]	3.060	0.097	4.270	1.030
a/L_n (D)	1	3.060	0.097	4.270	1.030
ν_e	[0-0.1]	**0.351**	0.043	0.057	0.023

Table 1: Table showing shaping parameters and gradient in the four cases considered. † Varied Consistently with β

Previous work found that increasing NBASIS_MAX improved agreement between TGLF and the gyrokinetic code GS2 for 4 radial cases of the T3D relaxed STEP scenario STEP-EC-HD [9] [7] (TGLF V1). However, a high filtering setting was necessary to match growth rates for the R4 radial case. Disabling width search and reducing NBASIS_MAX removes the need for aggressive filtering and improves agreement (TGLF V3) table 2.

3 Linear Comparison

Numerical Parameters	Default	V1	V3
NBASIS_MAX	4	10	4
WIDTH	1.65	1.9	1.3
NXGRID	16	32	32
THETA_TRAPPED	0.7	0.57	0.7
FIND_WIDTH	ES	ES	F

Table 2: Comparison of TGLF numerical parameters.

V3 improves the agreement particular at low k_y due to the removal of spurious low width KBMs Fig. 2b and clearly demonstrates β' stabilisation

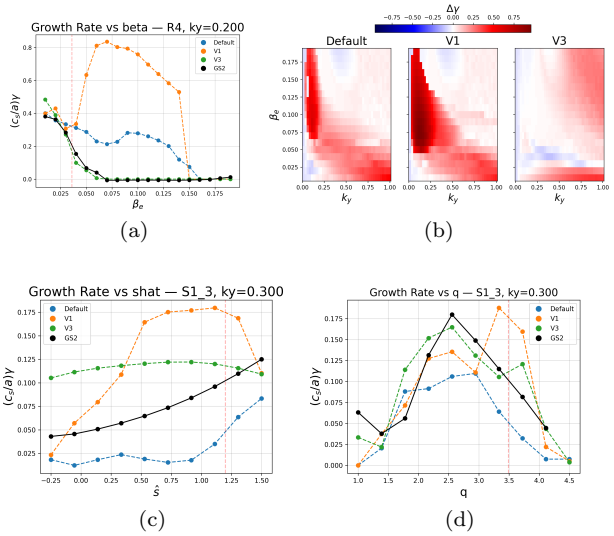

Figure 2: (a): Growth rate against β_e (β' varied consistently) plot for the R4 radial case at $k_y\rho_s = 0.2$. (b): Colour heatmap of absolute error in growth rates relative to GS2 for each TGLF version. (c) & (d) Growth rate plots for the STEP-EC-HD case against $\hat{s}$ and q respectively. The red vertical lines show the reference values

Fig. 2a. In the R3 and MAST-U case V3 has lower absolute error in growth rate as shown in table 3, with only marginally reduced agreement in the STEP-EC-HD cases at reference values. V3 more closely matches the effects of varying the q for the STEP-EC-HD case Fig. 2d, although a demonstration of increasing $\hat{s}$ disestablishing KBMs is absent Fig. 2c. Varying q is expected to move the beta prime stability boundaries, moving turbulence towards the first stability region at low q and second stability region at high q. When compared across a dataset based on the STEP-EC-HD geometry Fig. 3, V3 has reduce root mean square error, 28% vs 33%, in it's prediction of the growth rate.

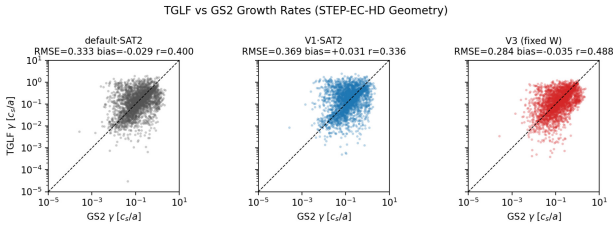

Figure 3: Comparison of TGLF growth rate against GS2 for 3000 data points generated from the STEP-EC-HD geometry. 7 parameters were varied including: q, $\hat{s}$, β, ν_e, electron temperature and density gradients and ion temperature gradient. Points were varied sampled at ky values ranging from 0.05 and 1

Case	Field	Version		
		Default	V1	V3
MAST-U 48567	γ	0.585	0.739	0.390
	ω	1.620	2.140	1.740
R3	γ	0.059	0.102	0.052
	ω	0.335	0.574	0.307
R4	γ	0.291	0.330	0.352
	ω	0.972	0.915	1.180
STEP-EC-HD	γ	0.041	0.072	0.054
	ω	0.373	0.783	0.412

Table 3: Mean absolute error in growth rate and mode frequency for each case and TGLF version.

4 Heat Flux Comparison

TGLF couples its gyrofluid linear solver with 3 options for a saturation rule, [10] [11] [12] which estimate the flux amplitude from the linear growth rate spectrum. $E \times B$ shear is modelled as a damping in the growth rate spectrum before the saturation rule is applied. Since all saturation rules require a peak in the γ/k_y spectrum, TGLF's ability to accurately resolve nonlinear fluxes is tied to its ability to generate this feature.

$E \times B$ shear scans for the MAST-U case 48507 and the STEP-EC-HD case were conducted, using the gyrokinetic code GENE. This is compared to TGLF quasilinear heat flux prediction using SAT 1 and SAT3 Fig. 4a & Fig. 4b. Width search is coupled with Saturation rule with SAT 1 forcing electromagnetic width search and SAT 3 electrostatic.

TGLF V1 with Sat 1 performs best in the STEP-EC-HD case Fig. 4b. V3 performs poorly in the STEP-EC-HD case predicting full turbulence sup-

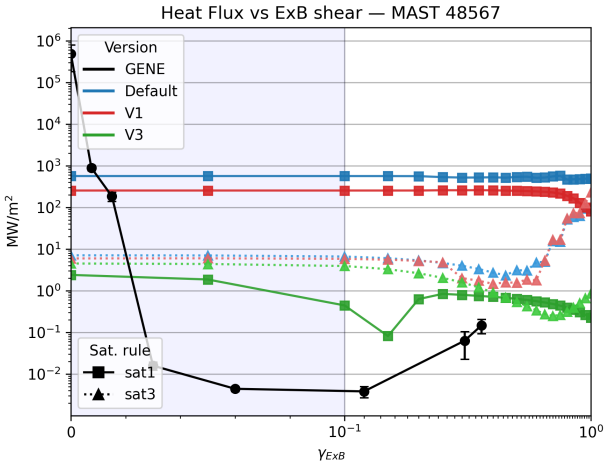

(a)

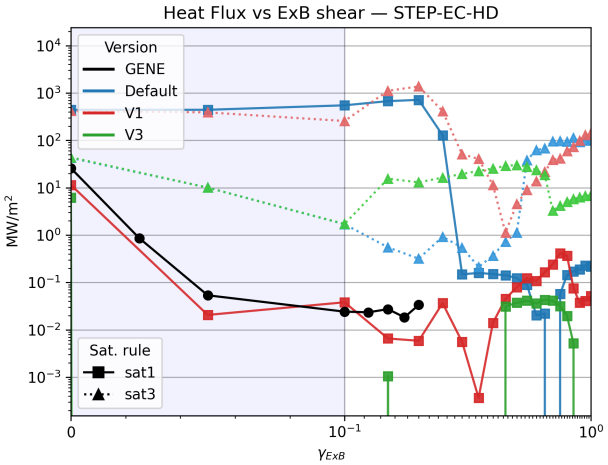

(b)

Figure 4: Plot of heat flux against $E \times B$ shear rates for (a): MAST-U shot 48567 (b): STEP case STEP-EC-HD. TGLF with different numerical settings are compared to a GENE nonlinear gyrokinetic simulation.

pression at finite $E \times B$, whilst all TGLF settings fail in the MAST-U case Fig. 4a

5 Conclusion

Improvements to TGLF's numerical settings have demonstrated an improvement in TGLF's ability to replicate β' stabilisation and the $E \times B$ shear stability threshold in spherical tokamak equilibrium from both MAST-U and STEP cases. TGLF V3 shows better linear agreement quantitatively with GS2, with large improvements found at low k_y values. However, the ability of TGLF to replicate the stability threshold for $E \times B$ shear whilst improved, is not sufficient. Whilst flatly multiplying the $E \times B$ shear value used in TGLF is an option, it greatly reduces the generality of the model. It is expected that a new saturation rule is needed to properly capture the effects of $E \times B$ shear in high β plasmas.

This work supported by the Engineering and Physical Sciences Research Council [EP/Y035062/1].

References

[1] Y. K. M. Peng and D. J. Strickler. In: 26.6 (Jan. 1986).

[2] Y. K. Peng. Tech. rep. Oak Ridge National Lab. (ORNL), Oak Ridge, TN (United States), Feb. 1985.

[3] D. Kennedy et al. In: 63.12 (Nov. 2023), p. 126061.

[4] C. Bourdelle et al. In: 58.1 (Nov. 2015), p. 014036.

[5] G. M. Staebler et al. In: 14.5 (May 2007), p. 055909. eprint: https://pubs.aip.org/aip/pop/article-pdf/doi/10.1063/1.2436852/13888907/055909_1_online.pdf.

[6] A. Najlaoui et al. In: 67.4 (Apr. 2025), p. 045016.

[7] B. Patel et al. In: ().

[8] M. ROMANELLI et al. In: 9 (2014), pp. 3403023–3403023.

[9] M. Giacomin et al. In: 91.1 (Feb. 2025), E16.

[10] G. M. Staebler et al. In: 23.6 (June 2016), p. 062518. eprint: https://pubs.aip.org/aip/pop/article-pdf/doi/10.1063/1.4954905/15908566/062518_1_online.pdf.

[11] G. Staebler et al. In: 61.11 (Sept. 2021), p. 116007.

[12] H. Dudding et al. In: 62.9 (July 2022), p. 096005.